TOPICAL REVIEW — High pressure physics

High pressure x-ray diffraction techniques with synchrotron radiation*

Jing Liu(刘景)†

Institute of High Energy Physics, Chinese Academy of Sciences, Beijing 100049, *China*

(Received 4 March 2016; published online 3 June 2016)

This article summarizes the developments of experimental techniques for high pressure x-ray diffraction (XRD) in diamond anvil cells (DACs) using synchrotron radiation. Basic principles and experimental methods for various diffraction geometry are described, including powder diffraction, single crystal diffraction, radial diffraction, as well as coupling with laser heating system. Resolution in d-spacing of different diffraction modes is discussed. More recent progress, such as extended application of single crystal diffraction for measurements of multigrain and electron density distribution, time-resolved diffraction with dynamic DAC and development of modulated heating techniques are briefly introduced. The current status of the high pressure beamline at BSRF (Beijing Synchrotron Radiation Facility) and some results are also presented.

Keywords: high pressure, x-ray diffraction, synchrotron radiation, diamond anvil cell

PACS: 61.05.cp, 07.35.+k, 07.85.Qe, 07.20.Ka **DOI:** 10.1088/1674-1056/25/7/076106

1. Introduction

Since the late 1970s, high-pressure (HP) synchrotron research has become a fast growing field. Over the past few decades, various HP experimental techniques based on synchrotron radiation have been successively developed, including HP x-ray diffraction (XRD), HP x-ray spectroscopy (XRS), HP inelastic x-ray scattering (IXS) , HP x-ray imaging, etc. In these techniques, XRD is the most common technique for high-pressure investigations and has been widely used for *in situ* determination of the structure and properties of materials.

Combining pressure vessels, like diamond anvil cells or large volume press, with synchrotron beamlines allows *in situ* XRD measurements under high pressure. The most commonly used HP apparatus for XRD is the diamond anvil cell (DAC) which is capable of generating pressures beyond 400 GPa[1,2] and is transparent to x-ray radiation. At ultrahigh pressures, the sample volumes are minute. In the megabar (1 megabar = 100 GPa) pressure range, sample dimensions in a DAC are typically less than 30 μm, so x-ray beams with sufficient intensity and minute size are needed in HP XRD measurements. The x-rays emitted from a synchrotron radiation source are ideally suitable for HP XRD studies, because the high brightness and high collimation of synchrotron radiation (SR) allow the x-ray beams to be focused down to micrometer-sized spots for probing minute samples at ultrahigh pressures. Additionally, high energy of SR is capable of penetrating surrounding vessel materials and suppressing background signals, which is crucially important for high quality diffraction data.

A number of beamlines have been built for HP XRD in synchrotron facilities in the world. Development of these techniques can be found in some of the literature.[3–7] The first HP XRD experiment integrated with synchrotron technique was pioneered at Hasylab in 1977 by Buras *et al.*[8] Since then the XRD using SR has become the main means of pressure-induced structural phase transition studies. In the 1980s, a number of beamlines at the first-generation or second-generation synchrotron facilities, such as DESY (Deutsches Elektronen Synchrotron),[9] CHESS (Conrell High Energy Synchrotron Source),[10,11] SSRL (Stanford Synchrotron Radiation Lightsource),[12,13] photon factory,[14] SRS (Synchrotron Radiation Source, Daresbury),[15] were reported to work for HP XRD studies. The energy dispersive x-ray diffraction (EDXRD) mode was mainly used in these beamlines and the synchrotron x-ray was incoming from the banding magnets. With the development of insertion devices (ID) techniques in SR facilities, some wiggler beamlines have been built for HP XRD studies.[16–19] The x-ray flux from wiggle is several orders of magnitude higher than the bending magnet which greatly improves the quality of data and reduces the measurement time. In the early 90s, the advent of area detectors resulted in fast progress and broader applications of angle-dispersive diffraction (ADXRD) methods in HP research.[16,17,20–22] In contrast, higher-resolution

*Project supported by the National Natural Science Foundation of China (Grant Nos. 10875142, 11079040, and 11075175). The 4W2 beamline of BSRF was supported by the Chinese Academy of Sciences (Grant Nos. KJCX2-SW-N20, KJCX2-SW-N03, and SYGNS04).

†Corresponding author. E-mail: liuj@ihep.ac.cn

© 2016 Chinese Physical Society and IOP Publishing Ltd

ADXRD methods employing CCD (charge couple device) or IP (image-plate) detectors allow high-resolution measurements that make powder refinement techniques possible up to the megabar (Mbar) pressure range.

There is no doubt that the development of HP XRD techniques benefit from the progress of synchrotron radiation light source. High brilliance of the third generation x-ray synchrotron sources greatly improved the size and the intensity of the x-ray beams available for experiments under extreme static pressure and temperature conditions. The development of x-ray diffraction in DACs involves the coupling of laser heating techniques.[23,24] A lot of high pressure diffraction beamlines have been equipped with laser heating DAC (LHDAC) systems at various synchrotron facilities in the world.[25–31] *In situ* measurements at high P–T gave a second variable in XRD data acquisition, providing us with various important information on the behavior of materials. Recently, x-ray powder diffraction in DAC has been extended with the introduction of radial diffraction (RXRD) geometry. This technique together with lattice strain theories[32–35] provides useful information about the strength, elasticity, deformation and rheology.[36–43] Single crystal XRD was first applied to HP using the EDXRD technique,[44,45] in which only the peak energy and peak orientation have been used for the determinations of unit-cell parameters but the peak intensities needed for complete structure refinements have not been used. Recently, single-crystal XRD using monochromatic beam and area detector has got rapid development, in which orientations and intensities of diffracted beams are measured. Some beamlines for high pressure research in the world have established routine procedures for conducting HP single crystal XRD experiments.[46–48] Using this technique, in addition to the structural measurements, information of electron density distribution can be obtained.[49,50] Very recently, emerging fast x-ray detectors, such as Pilatus, have brought new opportunities to HP XRD. Combined with a dynamic DAC (dDAC), which enables fast compression and decompression of sample in DACs, it is possible to study the time dependent phenomena in the regions of compression rates between the static technique and dynamic shock-driven devices.[51]

In this paper, the developments of HP diffraction techniques using synchrotron radiation in the diamond anvil cells is summarized. Basic principles and general setup for various HP diffraction experiments are described, including the powder diffraction, single crystal diffraction, radial diffraction, and laser heating diffraction. Resolution in d-spacing of EDXRD and ADXRD is analyzed, respectively. Recent results on BSRF (Beijing Synchrotron Radiation Facility) 4W2 beamline are also included. More recent developments of single crystal diffraction technique are briefly introduced.

2. HP diffraction techniques using synchrotron radiation

2.1. Synchrotron beamline for HP diffraction

Many synchrotron facilities in the world have beamlines dedicated to high pressure investigations. The most common experimental method is x-ray diffraction with diamond anvil cells. A dedicated beamline for HP diffraction in DACs is required to have certain abilities: (i) providing the x-ray with high brilliance in the higher energy range, (ii) focusing the divergent incident x-ray beam into the minute sample region, (iii) precise positioning and alignment of the sample and x-ray beam, even laser beams, (iv) collecting the diffraction signal with higher signal to noise ratio.

The scattering signal from the sample in DAC is very weak due to its "minute size and optical absorption of diamonds in the beam path. High intensity and high energy of incident x-ray are critical for obtaining effective diffraction information. Therefore, dedicated beamlines for HP diffraction are usually incoming from insertion devices, wiggler or undulator, which provide greatly enhanced brilliance and high photon energy. In the first- and second-generation synchrotron facilities wiggler is generally used.[15–19] Compared with bending magnets, a wiggler provides several orders of magnitude higher photon flux. Moreover, the continuous spectral distribution and wide energy range of a wiggler are especially suited for EDXRD, which is the prevailing method in early high pressure diffraction experiments. The third-generation synchrotron facilities based on undulators can provide a sufficient intensity of x-rays in the photon energy range from a few keV to 50 keV above.[52] Various HP XRD techniques with a monochromatic angle-dispersive mode have been rapidly developed in undulator beamlines.[53–56] With enhancement in source brilliance and the improvement in micro-focusing techniques, powder XRD have provided structural information with improved precision and accuracy up to multi-megabar pressures.

For the high pressure studies in diamond-anvil cells, sample dimensions are typically less than 30 μm in the megabar pressure range. Successful experiments critically depend on the ability to focus more photons into the minute sample region. A variety of techniques to focus hard x-rays to microbeam or nanobeam have been developed in conventional synchrotron beamlines, including the Fresnel zone plate,[57,58] Kirkpatrick–Baez (K–B) mirrors,[59–63] multilayer Laue lenses (MLL),[64] and compound refractive lens (CRL).[65] In the K–B optics arrangement, two independent grazing incidence mirrors are arranged with their surface normal nearly perpendicular to the incident x-ray and rotated 90° relative to each other. K–B mirrors can deliver a significantly higher x-ray flux and are capable of focusing x-rays with an energy range wider than 50 keV. For most of the high pressure

experiments, the focal spot sizes as small as a few microns are available. Another important constraint on the focusing for high pressure research is the requirement of working distance that should be sufficient to allow enough space for the DAC and other parts, such as the laser-heating carbon mirror. In contrast, it is the best choice to use K–B mirrors for micro-focusing in the high pressure diffraction beamlines.

The first x-ray diffraction apparatus used for high pressure research was developed at Beijing Synchrotron Radiation Facility (BSRF) in 1993.[66] For almost ten years, the HP diffraction at BSRF time shared a beamline with other stations. The experiments carried out in DACs used energy dispersive diffraction mode.[19,67] The dedicated beamline for high pressure research at BSRF was built in the early 2000s, which used an in-vacuum permanent magnetic wiggler (4W2) as the x-ray radiation source. Figure 1 shows the picture of 4W2 wiggler installed in Beijing Electron Positron Collider (BEPC), which provides flux of $\sim 10^{15}$ photons/s at 20 keV when the storage ring is run with electron energy of 2.5 GeV, current of 250 mA, and wiggle gap of 12 mm. The beamline started operation in the EDXRD mode and then stead of ADXRD. Figure 2 illustrates the current schematic of 4W2 beamline. The polychromatic x-ray is dispersed by a water-cooled double crystal Si (111) monochromator for selection of the required photon energy from the range 3.5–25 keV. According to the spectral distribution of 4W2, selecting the energy of 20 keV is appropriate for the high pressure experiments.

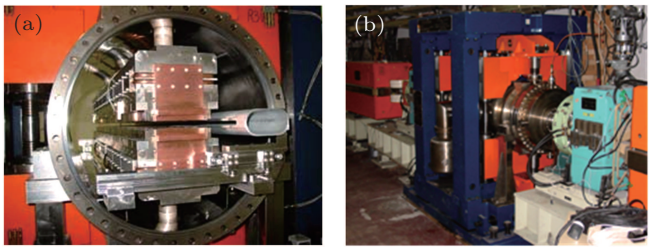


Fig. 1. (color online) Pictures of 4W2 in-vacuum wiggler at BSRF. (a) Inside view of wiggler, (b) installed in storage ring (Photos is provided by Shi C T).

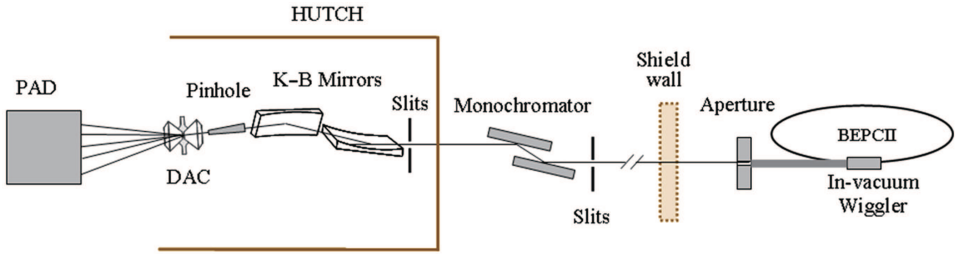


Fig. 2. (color online) Schematic diagram of the 4W2 beamline at BSRF.

We use two 100 mm long, actively bent mirrors in a Kirkpatrick Baez arrangement[59] to focus the monochromatic x-ray beam. The focusing quality depends mainly on the RMS slope error due to mirror misfiguring, static RMS slope error of the flat mirror and angular size of the source.[62,63] In the third generation synchrotron, high brightness (small angular divergence) of SR with sub-μrad slope errors of mirrors enables the focused beams to submicrometer size or smaller. As a first generation facility, the BEPC 4W2 has relatively large source size and large divergence. In our setup, the vertical mirror is only 18 meters from the source due to restrictions of the experimental hall space. In addition, the horizontal mirror cannot be very close to the sample because the high pressure vessels require a certain working distance. So it is difficult to focus the beam to several microns in size in the 4W2 beamline due to the large source size and small demagnification ratio. Focusing tests using 20 keV x-rays resulted in a double focused beam with a horizontal and vertical full width at half maximum (FWHM) of ~ 25 μm$\times 10$ μm, in which case the working distance is ~ 80 mm. With this beam size, a lot of diffraction measurements under a megabar have been successfully carried out.[68,69] Longer working distance is required for the laser heating experiments and will result in an increase in spot size.

2.2. HP diffraction techniques

The x-ray diffraction can determine the d-spacings of different lattice planes (hkl) and then solve the crystal structure by Rietveld refinement. The x-ray diffraction condition is described by the following Bragg equation:

$$\lambda = 2d\sin(\theta), \tag{1}$$

where λ is the x-ray wavelength, d is the crystallographic inter-planar spacing, and θ is the diffraction angle. Wavelength can be expressed as the function of energy: $\lambda = hc/E$, where h is the Planck constant, c is the speed of light, and E is the x-ray photon energy. The Bragg equation can be also expressed in the following:

$$E(\text{keV}) = 6.199/d\sin(\theta). \tag{2}$$

High pressure research involves the samples in different forms, for example, single crystal, polycrystalline, amorphous, and

liquid. For various sample forms, different HP XRD techniques have been developed, including powder XRD and single crystal XRD. With different incidence x-ray and data acquisition detectors, two distinct diffraction modes are used in high-pressure research: energy dispersive XRD and angle dispersive XRD. Figure 3 shows the schematic diagram of different XRD techniques.

2.2.1. HP powder diffraction

The powder diffraction is the most common technique in high pressure research and is suitable for any sample form except single crystal. The high pressure powder diffraction experiment can be carried out by energy-dispersive method (EDXRD) or angle-dispersive method (ADXRD). The early HP powder diffraction experiments mainly adopt energy-dispersive techniques. In EDXRD method, polychromatic x-rays are used as the primary beam, and the scattered photons are detected by a solid state detector (SSD) with energy resolution which is held at one fixed angle, 2θ, as shown in Fig. 3(a). Among SSDs, high purity germanium detectors are the most suitable for diffraction under high pressure, which provide an energy response of wide range, up to above 100 keV. The development of ADXRD technique benefits from the advent of area detectors. In the ADXRD configuration, the polychromatic x-rays from the source is monochromized by a monochromator and then impinges upon the sample. The diffraction patterns are recorded using an area detector with space resolution (also called 2D detectors), as shown in Fig. 3(b). According to the Bragg equation, the energy of the x-ray is fixed and the d-spacings of different lattice planes (hkl) are determined by the diffraction angle. Widely used 2D detectors are image plate (IP) and charge-coupled device (CCD). Recently the advent of fast pixel array detectors (PAD), such as Pilatus, makes the time-resolved high pressure XRD measurement possible.

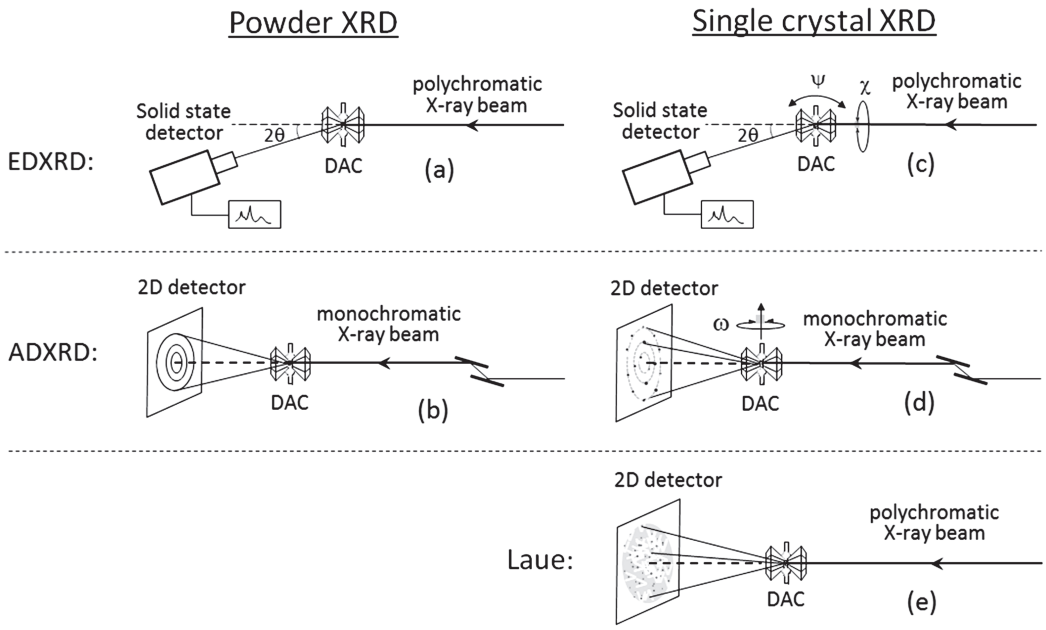


Fig. 3. Different diffraction geometry used with diamond anvil cell. (a) and (c) EDXRD, (b) and (d) ADXRD, and (e) Laue.

A critical factor determining the quality of diffraction data is the resolution, $\Delta d/d$ (d is the d-spacing, and Δd its uncertainty). From Bragg equation, the uncertainty in the d-spacing determination depends on the deviations of Bragg angle, $\Delta\theta$, and of x-ray energy, ΔE as follows:

$$\frac{\Delta d}{d} = \cot\theta\Delta\theta + \frac{\Delta E}{E}, \tag{3}$$

where $\Delta\theta$ is mainly caused by the angle divergence of the incident x-ray beam, ΔE is mainly from the energy resolution of solid-state detector in EDXRD, or of monochromator in ADXRD. Energy-dispersive diffraction is a low-resolution method. The lower resolution of EDXRD mainly comes from intrinsic properties of solid-state detectors. For example, the typical resolution of a germanium detector is ~ 150 eV at energy of 5.9 keV. Although the divergence of x-ray can be reduced with extremely good collimation of the incident beam the intrinsic lower energy resolution of solid-state detectors leading to the resolution in EDXRD is typically at $\Delta d/d \sim 10^{-2}$.[8,10] In ADXRD the contribution of energy resolution to the deviation is negligible. Usually the energy resolution of a monochromator easily reaches less than 10^{-4}. The uncertainty in the d-spacing determination is mainly from the divergence of the incident beam. In the use of K–B mirrors the divergence of the focusing beam is typically at milliradian which causes $\Delta d/d \sim 3\times 10^{-3}$. Reducing the acceptance of K–B mirrors can decrease the divergence of the incident beam, but the cost is the photon throughput weakening. Moreover, spatial reso-

lution of the 2D detector is also an impact factor. The angular broadening of in detecting systems is related to the detector pixel size and the distance between detector and sample as

$$\Delta\theta \approx \frac{w\cos^2(2\theta)}{L}, \tag{4}$$

where w is the pixel size of the detector and L is the distance between the detector and the sample. The spatial resolution of two-dimensional detectors is about 100 microns. The detector is usually located at the position where the detector can accept all diffraction lines from a DAC opening angle. For example, with a Mar-345 imaging plate and a symmetric DAC the distance of 250–300 mm is suitable. Further improvement of the resolution detector with small pixel size is expected. Increasing the distance between the detector and the sample can also improve the resolution, but it is difficult to break through the limitation of 10^{-3}. So in ADXRD the typical $\Delta d/d$ resolution of 3×10^{-3}–5×10^{-3} [56] which is in general adequate for studying simple structured materials at HP conditions. As an example, the difference in resolution between ADXRD and EDXRD is illustrated in Fig. 4.[70] Additionally, it is obvious that the relative intensity of (211) diffraction peak is much weaker using EDXRD than ADXRD due to the strong absorption of diamonds below 10 keV. In this example, the x-ray energy of 20 keV was used in ADXRD.

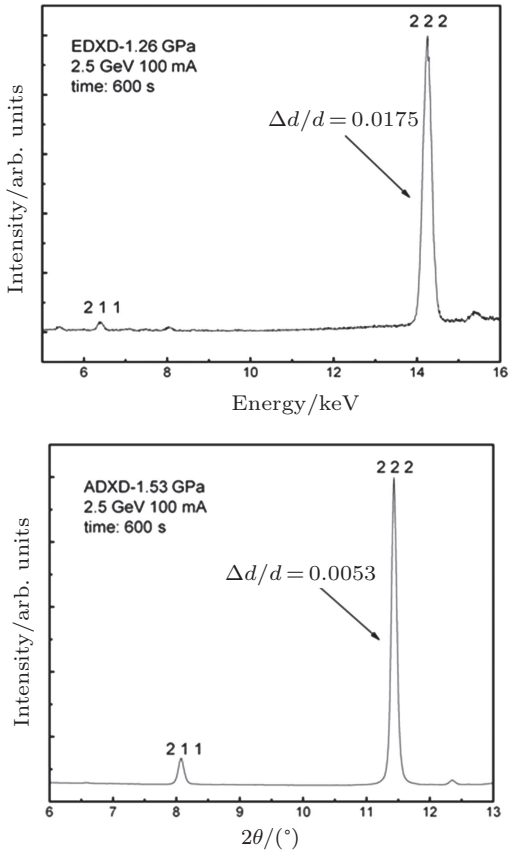


Fig. 4. Diffraction profiles obtained from the same sample of Gd_2O_3 using energy-dispersive (a) and angle-dispersive (b) techniques. The patterns were recorded at 4W2 beamline of BSRF.[70]

In spite of low resolution of EDXRD, it has been particularly useful for studying weakly scattering materials such as amorphous, liquid materials, and low-Z materials.[71–73] The advantage of this method is the excellent collimation, through which background scattering from surrounding materials (e.g., anvil, gasket, and medium) can be largely eliminated. Even though recently the energy dispersive diffraction mode has been replaced by the angular dispersive method in many HP beamlines, EDXRD is still an effective technique.

2.2.2. HP single crystal diffraction

Powder x-ray diffraction is a well-developed crystallographic technique with synchrotron HP beamlines and widely used for high pressure research. Nevertheless, this technique has some intrinsic shortages, such as the overlapping of diffraction peaks, strong preferred orientation, low resolution, low ratio of signal to noise, and so on. In particular, positional information on reflections is lost to a great extent in powder diffraction, and thus full structural characterization is usually difficult for phases existing only under high-pressure conditions. Single crystal x-ray diffraction can measure three-dimensional data and there are no peak overlaps or preferred orientation problems, which provides more precise structural information than powder diffraction. From single crystal data, space groups and a structural model can be unambiguously determined. Single crystal x-ray diffraction has many advantages in resolving some very complex crystallographic structure.[74] In addition, the problem of weak diffraction intensity from light element materials can be partially overcome by the use of the single-crystal x-ray technique. The concentration of diffracted intensity in single-crystal reflections allows the measurements on some low-Z materials at very high pressures,[44,45,75] which is difficult to achieve using powder diffraction.

The collecting of single crystal diffraction data at pressures in an HP beamline can adopt EDXRD, ADXRD or Laue methods, as shown in Fig. 3. The Laue method is the oldest diffraction technique for single crystals and it offers the simplest experimental process. This approach does not require rotation of the sample, as shown in Fig. 3(e). With the combination of the polychromatic radiation and an area detector all Laue spots from DAC access are collected simultaneously. Single crystal XRD was first used for high pressure research using the EDXRD technique.[44,45] In this method, polychromatic x-ray beam is used and a point detector records the diffraction patterns, as shown in Fig. 3(c). With fixed 2θ angle and a combination of ω and χ rotations, all crystallographic planes within the limits of the diamond cell window and ω angle can be brought into diffraction orientation. A

computer searching program is used to determine the orientation of the crystal.[18] Recently, monochromatic x-ray beam has been widely used in HP single crystal XRD with an area detector.[7,48,49] During diffraction patterns collection the sample is only rotated along a vertical axis perpendicular to the x-ray beam, marked as ω in Fig. 3(d). A procedure using step-scan covering a range of ω-rotation is performed to record individual images at specific rotation angles (ω). The scan range of ω is limited by the geometrical opening cone of the DAC, and the rotation step mainly depends on the experimental requirements, for example $-0.5°$–$2°$.[50,76]

In single crystal XRD, the relative intensities of different Bragg reflections are measured. It is essential that the sample volume illuminated by the x-ray beam remains constant when the sample is rotated around ω and χ in the x-ray beam.[77] Carefully selecting the relative sizes of the incident beam and the sample crystal can achieve this criteria. There are two ways to choose depending on the ability of micro-focusing. In third-generation synchrotron facilities, with the developments in micro-beam technology x-ray beams can be focused down to a size comparable with single crystal grain (typically several microns). Usually the decision is that the crystal is larger than the incident x-ray beam. For example, on the 16-BM-D beamline at the advanced photon source (APS), the focused beam size is about 5 μm×10 μm full-width half-maximum (FWHM) in both horizontal and vertical directions, respectively.[56] The single crystal is normally cut into rectangular pieces with section size of approximately 20 μm×30 μm.[50] With this method, the illuminated volume of the crystal will change during the sample rotation. The correction of volume is needed in data analysis. Another method is adopting a larger x-ray beam which completely covers the smaller sample crystal. It is commonly used at first- or second-generation synchrotron light sources where the x-ray beam is not easy to focus so small. For example, on the 4W2 beamline at the BSRF, the focus beam size is close to 30 μm (FWHM) in the horizontal with K–B mirrors. The size of single crystal sample is usually smaller than 20 μm. In all cases, it is essential to ensure that the x-ray beam is centered on the sample crystal.

Single-crystal diffraction techniques have been developed at the high pressure beamline 4W2 at the BSRF. The sketch of the experimental set-up is shown in Fig. 5. The ADXRD method is used and the diffraction data from single crystals at high pressure are collected by an image plate detector (MAR345). A DAC specially designed with a large opening (70°) was used for a large coverage in reciprocal space. During data collection the DAC is only rotated around the ω axis. Because the source size of 4W2 is larger and the sample position is limited in $\sim$ 18 m from the source, it is difficult to focus the incident beam to a size comparable with single crystal grains. So the larger incidence beam than the single crystal sample is used during the single crystal data acquisition. Sometimes a non-focusing beam is used to reduce the divergence angle. With a combination of slits and the pinhole, the non-focusing beam is reduced to the dimensions of 50 μm × 50 μm which can completely cover the single crystal with size of the $\sim$ 20 μm as the step-scan is performed. Between the DAC and the pinhole, a transmittance photodiode is mounted to monitor the incidence beam intensities which will be used for intensity correction during the data processing. A lead shielding plate with a 5 mm diameter aperture is used to shadow stray light and minimize the general background level. A software package HPSXD has been developed to control the collecting of XRD images and data processing. In this package, a new algorithm can be used to handle the multi-particle diffraction data.[47] Using this system, the HP diffraction data from several single crystals have been collected and with the maximum entropy method, the information of electron density distributions has been obtained.

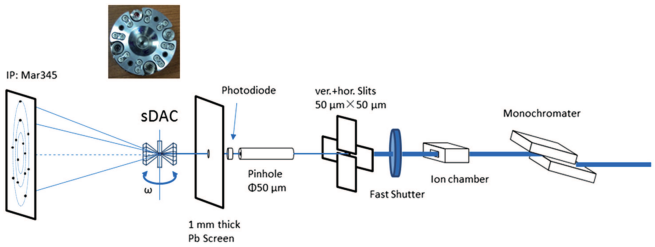


Fig. 5. (color online) Schematic layout of beamline components for HP single crystal diffraction at BSRF (supported by Hui Li). Insert is a specially designed DAC for single crystal diffraction.

2.2.3. HP radial diffraction

The diamond anvil cell is a uniaxial stress device, as shown in Fig. 6. According to the lattice strain theory developed by Singh *et al.*,[32–35] the stress state of a sample in the diamond anvil cell can be described by a maximum stress along the cell loading axis, σ_3, and a minimum stress in the radial direction, σ_1. The hydrostatic stress component is related to σ_3 and σ_1, by $\sigma_P = (\sigma_3 + 2\sigma_1)/3$. The difference between σ_3 and σ_1 is termed as the uniaxial stress component t,

$$t = \sigma_3 - \sigma_1. \tag{5}$$

The existence of differential stress, t, makes the samples in DAC always subjected to a nonhydrostatic compression which can strongly affect the measured lattice strains. Although the quasihydrostatic conditions can be obtained with pressure medium around the sample, a completely hydrostatic

environment cannot be sustained above ∼ 15 GPa due to the freezing of all known pressure media. In the conventional diffraction experiments using a DAC, the primary x-ray beam passes parallel to the load axis, as shown in Fig. 7(a). In this case, the stress of the sample subjected is minimum at $\psi = 90°$ and maximum at $\psi = 0°$. The ψ is the angle between the diamond cell stress axis and the diffraction plane normal. In the DAC diffraction experiments, Bragg angle θ is usually ∼ 15°. Thus x-ray diffraction measurements are confined to near the minimum strain direction, and the observed lattice strain is smaller than the strain component due to the hydrostatic pressure. The result is that the observed compression curve always biases the hydrostatic curve.[79–81] By using an x-ray transparent gasket in the diamond anvil cell, such as beryllium and amorphous boron, a novel diffraction technique unlike conventional geometry has been developed, which is called radial XRD (RXRD).

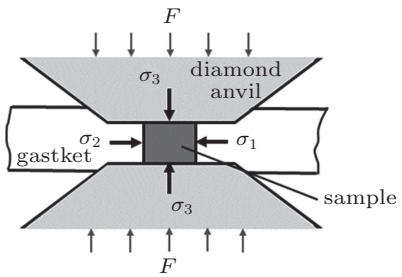


Fig. 6. Stress state of the uniaxially compressed sample in a diamond anvil cell.

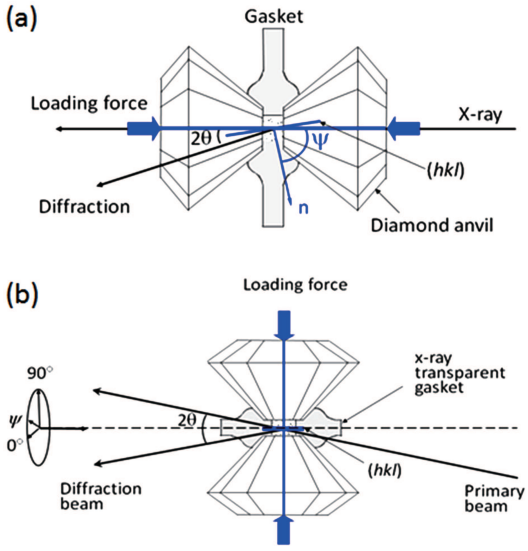


Fig. 7. (color online) (a) Axial x-ray diffraction geometry; (b) radial x-ray diffraction geometry.

In the radial diffraction geometry, the primary x-ray beam passes in close to perpendicular to the load axis direction, as shown in Fig. 7(b). The radial XRD allows measurements of lattice strains at any orientation relative to the stress axis if rotating DAC. The measured d-spacing for a given set of lattice planes, $d_m(hkl)$, is a function of the angle ψ

$$d_m(hkl) = d_p(hkl)[1 + (1 - 3\cos^2\psi)Q(hkl)], \tag{6}$$

where $d_p(hkl)$ is the d-spacing that would result under the application of hydrostatic pressure σ_P alone, and $Q(hkl)$ is the lattice strain under the uniaxial stress condition.[33,82] The terms $d_p(hkl)$ and $Q(hkl)$ can be determined from Eq. (6) using $d_m(hkl)$ versus ψ data. According to Eq. (6), $d_m(hkl)$ will vary linearly with $1 - 3\cos^2\psi$. It reaches a maximum at $\psi = 90°$ and minimum at $\psi = 0°$. The measured d-spacing at $\psi = 54.7°$ ($1 - 3\cos^2\psi = 0$) is the equivalent of that due to the hydrostatic component of stress. At this angle, there is no contribution to the measured d-spacing from the differential stress. Thus, it is possible to obtain a quasihydrostatic compression curve when the sample is subjected to highly nonhydrostatic stress states.[37,39,83,84]

Using the radial XRD technique together with lattice strain theories, it is also possible to obtain useful information that is unavailable with hydrostatic experiments, such as the strength, elasticity, rheology, and texturing. The slope $Q(hkl)$ in Eq. (6) is a constant for elastically isotropic materials, but varies with hkl for elastically anisotropic materials. When the aggregate polycrystalline sample in the diamond anvil cell is assumed under isostress conditions the uniaxial stress component t can be expressed as[34,35]

$$t = 6G\langle Q(hkl)\rangle, \tag{7}$$

where $\langle Q(hkl)\rangle$ represents the average $Q(hkl)$ value over all observed reflections, and G is the aggregate shear modulus of the polycrystalline sample. The von Mises yield criterion suggests: $t = 2\tau = Y$, where τ is the shear strength and Y is the yield strength of the sample. In fact, t could be less than the yield strength. If the differential stress t has reached its limiting value of yield strength at high pressures, $6\langle Q(hkl)\rangle = t/G$ will reflect the ratio of yield strength to the shear modulus. Using Eqs. (6) and (7) the lattice strain theories have been successfully applied to determine the strength, elasticity and rheology of materials from the radial x-ray diffraction data under uniaxial compression.[85–90]

Both radial XRD techniques using EDXRD and ADXRD respectively have been developed at BSRF. In energy-dispersive RXRD experiments, the diffracted intensity was recorded using a Ge solid-state detector with a fixed angle, 2θ. The diamond-anvil cell is mounted in a rotation stage whose axis bisects 2θ, as shown in Fig. 8. Both the incident and diffracted beams passed through the beryllium gasket which absorbs little of the high-energy x rays. The angle ψ between the diffraction plane normal and the cell-loading axis can vary from 0° (Fig. 8(a)) to 90° (Fig. 8(b)) by rotating DAC. At each pressure, energy-dispersive diffraction patterns were recorded at angular intervals, such as 5°–15°. The equivalent hydrostatic pressures were determined from the measured lattice parameter at $\psi = 54.7°$. Nonhydrostatic compression behavior of osmium (Os) was investigated up

to 58.2 GPa using this method.[91] To ensure maximum non-hydrostatic stresses, the sample was compressed without any pressure-transmitting medium. Selected x-ray diffraction patterns as a function of angle at 36.5 GPa and dependence of d spacing on $(1-3\cos^2\psi)$ for diffraction line (110) at different pressures are shown in Fig. 9. From radial diffraction data the strength, elastic moduli, as well as the apparent c/a ratio of Os were examined under nonhydrostatic compression and the hydrostatic compression curve has been rechecked at $\psi = 54.7°$.[91]

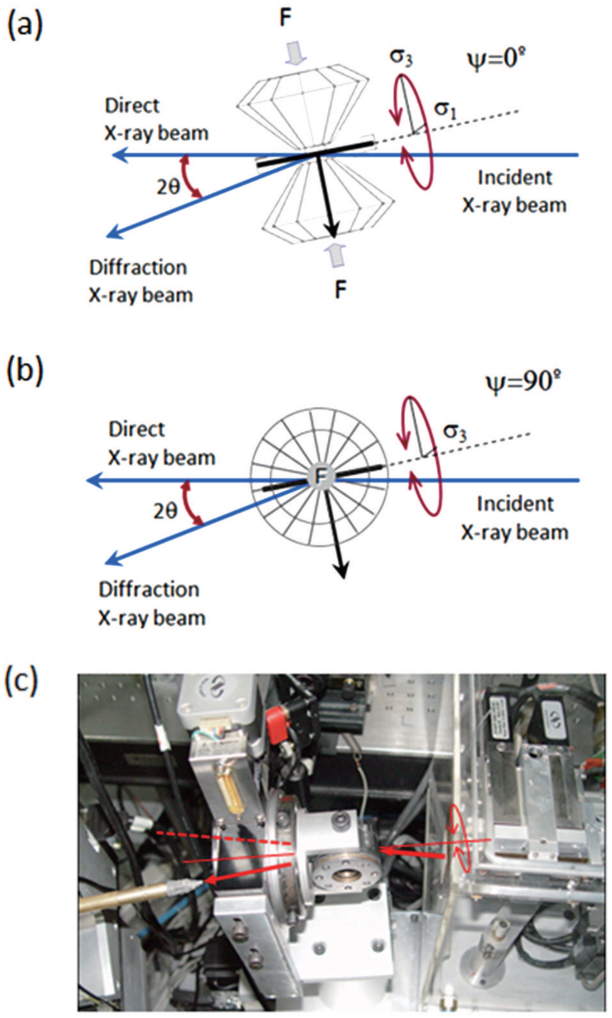


Fig. 8. (color online) Experimental geometry for energy-dispersive radial diffraction. The ψ is the angle between the diamond cell stress axis and the diffraction plane normal. (a) $\psi = 0°$, diffraction plane normal parallel to the diamond cell stress axis; (b) $\psi = 90°$, diffraction plane normal perpendicular to stress axis. (c) Photograph of experimental setup at BSRF, a symmetric DAC is used.

In a general angle-dispersive radial x-ray diffraction experiment, the incident x-ray is perpendicular to the compression axis and passes through a beryllium gasket, as shown in Fig. 10(a). The diffraction patterns were collected using an imaging plate orthogonal to the incident beam. The position of the diffraction lines and intensity of diffraction are analyzed as a function of the azimuthal angle δ. In order to determine the variations in the position of the diffraction peaks and their intensities with the azimuthal angle δ, the diffraction patterns are cut into small arcs of 2° to 5° and integrated with Fit2d. For each pattern, this produces between 90 and 36 segments with the diffraction intensity as a function of the diffraction angle 2θ for δ between 90° and 270°. The patterns are then fitted individually with Pseudo–Voigt line shapes using the software package Multifit 4.2. The fitted peak positions were used to calculate the d-spacings as a function of the azimuth angle.

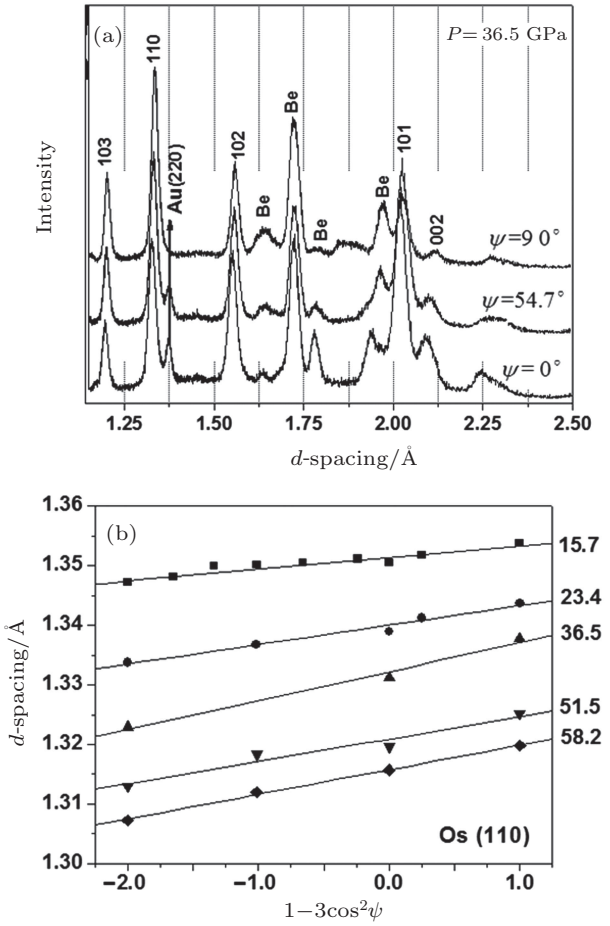


Fig. 9. Radial diffraction of osmium. (a) The x-ray diffraction patterns taken at $\psi = 0°$, 54.7°, and 90° under 36.5 GPa. (b) Dependence of d-spacing on $1-3\cos^2\psi$ for diffraction line (110). The solid lines are least-squares fits to the data. The pressure is determined from the lattice parameter of gold observed at $\psi = 54.7°$.[91]

The ψ corresponding to the angle between the diffracting plane normal and the loading axis is calculated using the equation[40]

$$\cos\psi = \cos\theta\cos\delta, \tag{8}$$

where θ is the diffraction angle and δ is the azimuthal angle in the plane of the detector. In order to minimize the contribution of Be diffraction lines to the sample patterns, the DAC can be tilted to an angle α as shown in Fig. 10(b). In this geometry, ψ can be calculated from

$$\cos\psi = \sin\alpha\cos\delta\cos\theta + \cos\alpha\sin\theta. \tag{9}$$

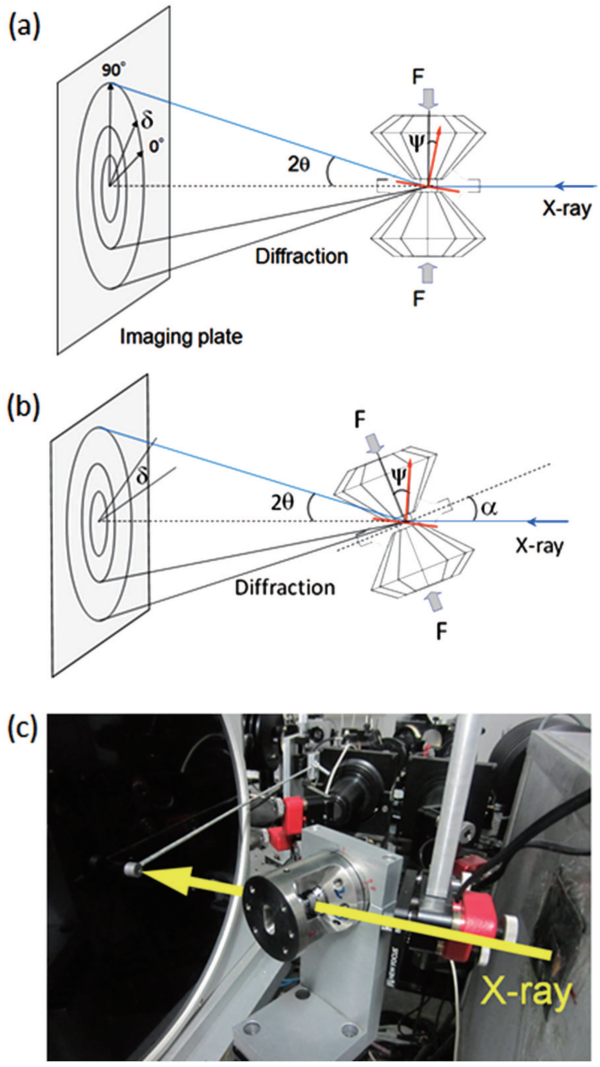


Fig. 10. (color online) Schematic of experiment for angle-dispersive radial diffraction. (a) Diffraction geometry: incident beam perpendicular to the compression axis; (b) diffraction geometry: compression axis tilts angle α; (c) photograph of experimental setup at BSRF, a panoramic DAC is used.

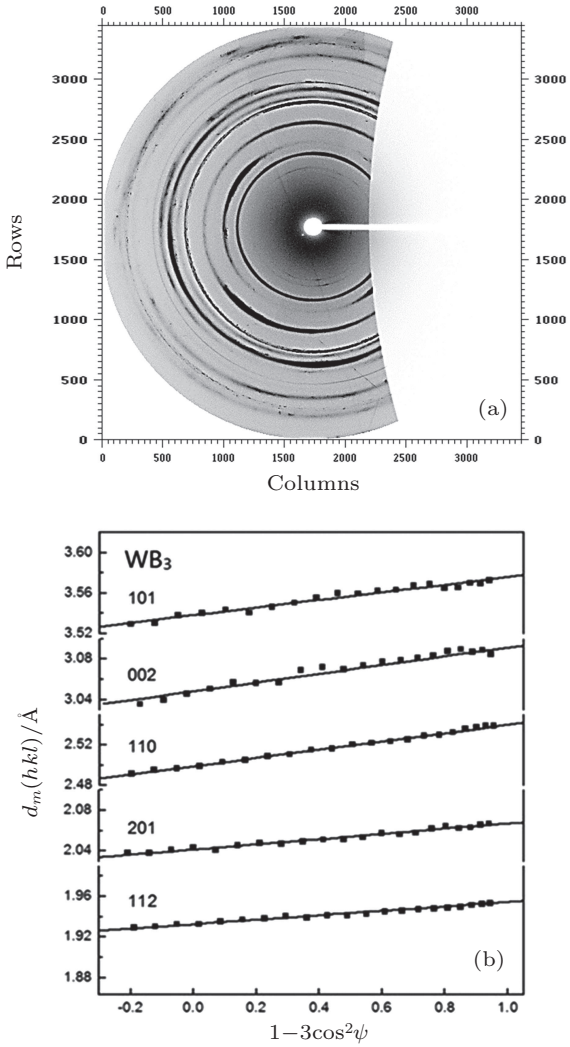


Fig. 11. (a) Angle-dispersive radial diffraction pattern of WB3 at 45 GPa. The DAC was tilted 28°; (b) the d-spacings versus $1-3\cos^2\psi$ for selected diffraction peaks of WB_3 at 45 GPa. The data were obtained with integrations over 5° intervals of the azimuth angle from 180° to 270°. The solid lines are least-squares linear fits to the data. The pressures are determined from the Mo (110) peak at $\psi = 54.7°$.[92]

As an example, a diffraction pattern of tungsten triboride (WB_3) from angle-dispersive radial diffraction is shown in Fig. 11(a).[92] The experiment was performed at BSRF with a panoramic DAC tilted 28°. The diffraction patterns were recorded on a Mar345 image-plate. At each increasing pressure, the pattern was collected after about 30 min to allow for stress relaxation. The plot of d-spacing as a function of $1-3\cos^2\psi$ for selected diffraction lines from the pattern at 45 GPa is shown in Fig. 11(b), which is obtained with integrations over 5° intervals of the azimuth angle from 180° to 270°. Using this technique together with the lattice strain theory, some compounds consisting of heavy transition metal and light element B, such as WB_x, MoB_x, have been studied.[93,94] These materials have been proposed to be potential superhard or ultrahard. Some information about the hydrostatic compression properties and strength has been obtained from the radial diffraction data.

2.2.4. HP diffraction at high temperature

An x-ray measurement at simultaneous pressure and temperature provides us with various important information on the behavior of materials and their crystal structures under extreme conditions. With further development and application of synchrotron light sources, an important extension of the high pressure experimental techniques using synchrotron involves the coupling of high or low temperature techniques with polycrystalline diffraction. These techniques provide an *in situ* measure of crystal structures at P–T conditions which provide fundamental information for understanding physical properties of materials.

Conventional diffraction systems with DAC can be readily combined with variable-temperature studies, including low-temperature cryogenic methods and high-temperature resistive heating techniques (both external and internal) as well as laser-heating methods. By using a continuous wave (cw)

laser heated diamond anvil cell (LHDAC), it is not difficult to heat the sample reaching much higher temperature ($T >$ 1500 K) at high pressure ($P >$ 100 GPa). Because of this advantage, many high pressure diffraction beamlines have been equipped with laser heating systems at various synchrotron facilities in the world.[26–31,95,96]

A typical configuration of x-ray diffraction combining with the laser heating technique in a high-pressure cell is shown in Fig. 12. For this technique, the sample in a DAC is directly irradiated by the laser beam with high power density. The choice of laser wavelength depends on the materials to be heated. For opaque materials, near infrared (IR) lasers, such as Nd:YAG (1.064 μm wavelength)[28,29,97] and Nd:YLF lasers (1.053 μm wavelength),[27,31] are usually used. Most optically transparent samples (silicates, oxides, and molecular phases) can be heated to reach the requisite temperatures directly using CO_2 lasers with a wavelength of 10.64 μm.[26] Another method available for heating transparent samples by near IR lasers is mixing powdered black platinum in small proportion ($\sim$ 10%) with the sample.[98] Black platinum is a good near IR laser absorber. It is crucial to produce uniform temperatures in the heating area of the sample for reliable experimental data. Employing double-sided laser-heating technique can reduce the sample temperature gradient axially,[99] in which the sample in DAC is irradiated from both sides by the high-power laser beam. To minimize the radial temperature gradient, the optimal power distribution of the laser beam is just the first step. Shen *et al.* have developed a laser heating system combining two YLF lasers in TEM_{00} and (donut) TEM_{01} modes to create a flat temperature distribution up to better than 1%.[27]

For *in situ* diffraction experiments on laser-heated diamond-anvil cell samples, a perfect alignment is required, with all heating laser beams, thermal radiation paths, incident x-ray beams, and characterizing systems aligned to the sample position within a few microns. The insert in Fig. 12 illustrates a typical arrangement for the sample in a laser-heating DAC. The x-ray beam should be much less in size than the heating spot to avoid signals from any cold part of the sample. The high brilliance of synchrotron radiation allows control of the x-ray beam to a size significantly smaller than that of the laser heating spot, but still with enough photon flux to accurately measure x-ray diffraction measurements. The x-ray beam size at synchrotron beam lines is typically less than 5 μm and the laser heated spot is often greater than 30 μm.

A double laser-heating system has been developed at 4W2 beamline of BSRF. Figure 13 shows the experimental setup for *in situ* diffraction at high pressure and temperature. The photo presents the earlier configuration with EDXRD mods but has now been replaced by ADXRD mode. Nd:YLF laser is used in the system. The laser heating spot is controlled to $\sim$ 50 μm because the focused x-ray beam is restricted to $\sim$ 20 μm due to large source size.

The laser heating technique with x-ray diffraction has evolved into a routine experimental method for *in situ* measurements under extreme conditions. Over the last decade, this technique has been widely used for high P–T studies such as phase transition studies,[23,100–104] high pressure melting,[103–108] syntheses of high P–T phases,[109–112] and P–V–T equations of state.[28–31] Recently, the phase transition sequences of the rare earth manganites, indates and gallium garnets have been investigated in a laser-heated diamond anvil cell using synchrotron radiation x-ray diffraction at BSRF.[69,98,117–119] The studies provide more understanding of the phase transition mechanisms in these rare earth compounds at high pressure and temperature.

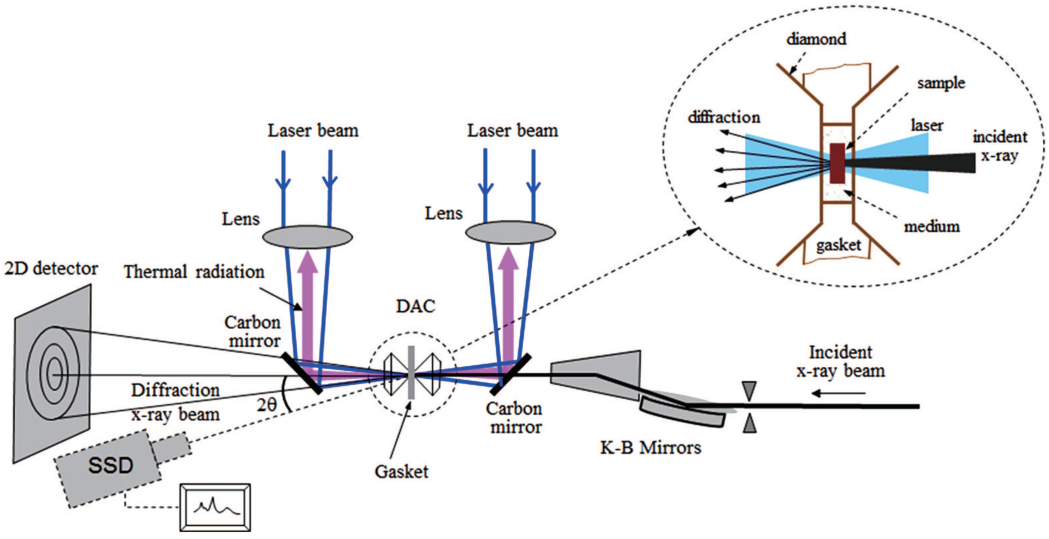


Fig. 12. (color online) A typical configuration of x-ray diffraction combining with a laser heated DAC.

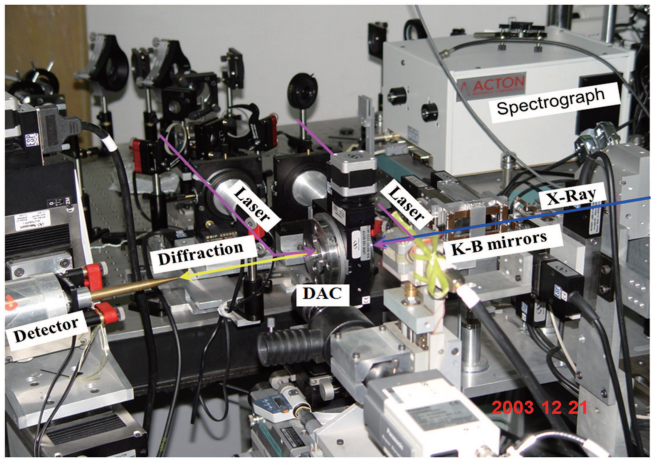


Fig. 13. (color online) The *in situ* experimental setup for high pressure and temperature diffraction. The figure shows an EDXRD system combined with the double-laser heating system in DAC. The spectrograph is used for temperature measurement.

2.3. Recent developments

With the developments of micro-beam technology in synchrotron radiation and the use of area detector, HP single crystal diffraction technique has been greatly developed in both measurements and applications. Single-crystal XRD provides the most precise structural information that can be used to uniquely determine the space group and structural model. However, a single crystal sample in a DAC is usually crushed into many particles under higher pressure. On the other hand, single crystals fail to survive after a pressure-induced phase transition. A common method for reformation of the single crystal is promoting grain growth by heating the sample in the high pressure phase but it often results in highly spotty XRD patterns. Therefore, so far the structural studies under higher pressure have been limited to powder diffraction techniques.

Newly developed multigrain single-crystal x-ray diffraction analysis technique in a diamond anvil cell can overcome these limitations. With the developments of microbeam technology in synchrotron radiation, the minimal size needed for single-crystal diffraction has been reduced to around 1 mm. Traditional powder sample may be treated as multiple grains. A novel analytical approach known as multigrain crystallography is applied for structure determination of multi-grain and the quality of the resulting refinements is comparable to single crystal work.[47,120] This method is applicable for samples with up to a thousand grains, a few hundred grains and about ten grains, respectively. The multigrain XRD is a very promising method for high pressure crystallography research and has been used in studies of deep Earth materials.[76,121]

The recent development of single crystal diffraction techniques has achieved a significant extension of the application for high pressure research. Over the past few decades, single crystal diffraction was mainly used for structure solution and refinement. Using the recently developed single crystal x-ray diffraction technique, besides the information on atomic arrangement the information on electronic structure under pressure can be obtained. By using the maximum entropy method (MEM), the resultant single crystal diffraction data has been used to determine the electron density distribution under high pressure.[49,50,78] Preliminary results in germanium suggest that the pressure-induced phase transformation is related to the electronic changes before the structural phase transition. This new capability of single crystal diffraction provides an approach to further understand the mechanism of electronic structure phase transitions.

So far, high pressure diffraction experiments in a DAC are mainly carried out at a static pressure condition, i.e., using opposed anvils to exert a fixed pressure on the sample. However, once the applied force is constant, the final pressure in the material studied is reached with a delay depending on the driving mechanism of DAC. This time dependence strongly influences the phase transformation pathways. Recently, a dynamic DAC (dDAC) has been developed for fast compression and decompression,[122,123] which uses electromechanical piezoelectric (PZT) actuators or pneumatic membrane to replace screws in the DAC. Various compression rate can be obtained by controlling the change speed of driving voltage (PZT) or gas-pressure (membrane). In particular, this capability covers the regions of compression rates between static techniques (DACs and large volume presses) and dynamic shock-driven devices (gas guns, explosive, and laser shock) that have been sparsely studied. Coupling dDAC with fast x-ray detectors, such as Pilatus and Eiger, time-resolve HP x-ray diffraction can be performed at various compression rates,[51] which allows studies of the kinetics of phase transitions, phase growth, and metastable phases.

Another development area is the modulated heating. Pulsed laser heating in diamond anvil cells has recently attracted interest.[123,124] The short heating duration can effectively suppresses thermally activated chemical diffusion and reaction, reaching even higher temperatures compared to continuous wave laser heating. A laser pulse can be synchronized with gated x-ray detector, such as Pilatus, and time-resolved radiometric temperature measurements. This new laser heating technique preserves a great potential for the accurate measurement of melting curves, phase transition relations, thermal diffusivity, and pressure-volume-temperature equations of state.

3. Summary

Recent advances at synchrotron radiation facilities have made the developments of various synchrotron techniques for high pressure research possible. Among these, x-ray diffraction remains the basic experimental method. With enhancement in source brilliance and the improvement in micro-

focusing techniques, powder XRD has provided structural information with improved precision and accuracy up to multi-megabar pressures. With the introduction of radial diffraction geometry, powder diffraction in DAC has been extended to measure strength, elasticity, deformation, and rheology of materials. HP single-crystal diffraction method using monochromatic beams and area detectors can provide accurate structure determination, as well as the information of electron density distribution. With the developments in micro-focusing technology in synchrotron radiation, a new crystallography for multi-grains data has been recently developed resulting in the quality of refinements comparable with single-crystal work. ADXRD provides improved resolution, typically at $\Delta d/d$ of around 3×10^{-3}–5×10^{-3}, which has become the dominant approach for structural studies at high pressure. Even so EDXRD is still particularly useful for studying weakly scattering materials such as amorphous, liquid materials and low-Z materials. Laser heating technique can couple with ADXRD or EDXRD and has evolved into a routine experimental method in HP beamlines that is widely used for high P–T studies such as phase transition studies, high pressure melting, syntheses of high P–T phases, and P–V–T equations of state. Recently emergence of fast gated detectors and development of dynamic DAC make the time-resolved XRD measurement under high pressure possible, which is a very promising approach for the future high pressure research. The XRD with synchrotron radiation has long been the dominant method for materials research under high pressure, and is likely to remain so in the future.

Acknowledgments

I would like to acknowledge Dr. Hui Li for useful discussion on the single crystal diffraction and providing a schematic diagram. Special thanks goes to Xiao-dong Li, Yan-chun Li and many colleagues for efforts in the construction of 4W2 beamline at BSRF.

References

[1] Akahama Y and Kawamura H 2007 *High Pressure Res.* **27** 473
[2] Dubrovinsky L, Dubrovinskaia N, Prakapenka V B and Abakumov A M 2012 *Nature Commun.* **3** 1163
[3] Paszkowicz W 2002 *Nucl. Instr. and Meth. Phys. Res. B* **198** 142.
[4] Hemley R J, Mao H K and Struzhkin V V 2005 *J. Synchrotron Rad.* **12** 135
[5] Mao H K and Mao W L 2007 *Treatise on Geophysics* (Amsterdam: Elsevier) p. 231
[6] Shen G and Wang Y 2014 *Rev. Mineral. Geochem.* **78** 745
[7] Lavina B, Dera P and Downs R T 2014 *Rev. Mineral. Geochem.* **78** 1
[8] Buras B, Olsen J S, Gerward L, Will G and Hinze E 1977 *J. Appl. Crystallogr.* **10** 431
[9] Olsen J S, Buras B, Gerward L and Steenstrup S 1981 *J. Phys. E: Sci. Instrum.* **14** 1154
[10] Baublitz Jr. M A, Arnold V and Ruoff A L 1981 *Rev. Sci. Instrum.* **52** 1616
[11] Brister K E, Vohra Y K and Ruoff A L 1986 *Rev. Sci. Instrum.* **57** 2560
[12] Skelton E F, Qadri S B, Webb A W, Lee C W and Kirkland J P 1983 *Rev. Sci. Instrum.* **54** 403
[13] Webb A W, Qadri S B, Wolf S A, Lacoe R C, Feldman J L, Elam W T, Carpenter Jr E R and Huang C Y 1984 *Rev. Sci. Instrum.* **55** 849
[14] Kikegawa T, Shimomura O, Iwasaki H, Sato S, Mikuni A, Iida A and Kamiya N 1989 *Rev. Sci. Instrum.* **60** 1527
[15] Pattison P, Cernik R J and Clark S M 1989 *Rev. Sci. Instrum.* **60** 2376
[16] Nelmes R J, Hatton P D, McMahon M I, Piltz R O, Crain J, Cernik R J and Bushnell-Wye G 1992 *Rev. Sci. Instrum.* **63** 1039
[17] McMahon M I and Nelmes R J 1994 *Mater. Sci. Forum* **166–169** 117
[18] Hu J Z, Mao H K, Shu J and Hemley R J 1994 *AIP Conf. Proc.* **309** 441
[19] Liu J, Che R Z, Zhao J, Jing Y H, Yang Y and Ju X 2001 *Nucl. Instrum. Meth. A* **467–468** 1069
[20] Shimomura O, Takemura K, Fujihisa, Fujii Y, Ohishi Y, Kikegawa Amemiya T Y and Matsushita T 1992 *Rev. Sci. Instrum.* **63** 967
[21] Nelmes R J and McMahon M I 1994 *J. Synchrotron Rad.* **1** 69
[22] Fujiwara A, Ishii K, Watanuki T, Suematsu H, Nakao H, Ohwada K, Fujii Y, Murakami Y, Mori T, Kawada H, Kikegawa T, Shimomura O, Matsubara T, Hanabusa H, Daicho S, Kitamura S and Katayama C 2000 *J. Appl . Cryst.* **33** 1241
[23] Boehler R 2000 *Rev. Geophys.* **38** 221
[24] William A B 2001 *Rev. Sci. Instrum.* **72** 1283
[25] Brister K and Bassett W 1995 *Rev. Sci. Instrum.* **66** 2698
[26] Fiquet G, Andrault D, Itié J P, Gillet P and Richet P 1996 *Phys. Earth Planet. Inter.* **95** 1
[27] Shen G, Rivers M L, Wang Y and Sutton S R 2001 *Rev. Sci. Instrum.* **72** 1273
[28] Andrault D and Fiquet G 2001 *Rev. Sci. Instrum.* **72** 1283
[29] Watanuki T, Shimomura O, Yagi T, Kondo T and Isshiki M 2001 *Rev. Sci. Instrum.* **72** 1289
[30] Yagi T, Kondo T, Watanuki T, Shimomura O and Kikegawa T 2001 *Rev. Sci. Instrum.* **72** 1293
[31] Meng Y, Shen G and Mao H K 2006 *J. Phys.: Condens. Matter* **18** s1097
[32] Singh A K 1993 *J. Appl. Phys.* **73** 4278
[33] Singh A K and Balasingh C 1994 *J. Appl. Phys.* **75** 4956.
[34] Singh A K, Mao H K, Shu J and Hemley R J 1998 *Phys. Rev. Lett.* **80** 2157
[35] Singh A K, Balasingh C, Mao H K, Hemley R J and Shu J 1998 *J. Appl. Phys.* **83** 7567
[36] Mao H K, Shu J, Shen G, Hemley R J, Li B S and Singh A K 1998 *Nature* **396** 741
[37] Duffy T S, Shen G, Heinz D L, Shu J, Ma Y Z, Mao H K, Hemley R J, and Singh A K 1999 *Phys. Rev. B* **60** 15063
[38] Shieh S R, Duffy T S and Li B S 2002 *Phys. Rev. Lett.* **89** 255507
[39] He D W, Shieh S R and Duffy T S 2004 *Phys. Rev. B* **70** 184121
[40] Merkel S, Wenk H R, Shu J F, Shen G Y, Gillet P, Mao H K and Hemley R J 2002 *J. Geophys. Res.* **107** ECV 3-1-ECV 3-17
[41] Wenk H R, Matthies S, Hemley R J, Mao H K and Shu J F 2000 *Nature* **405** 1044
[42] Merkel S, Kubo A, Miyagi L, Speziale S, Duffy T S, Mao H K and Wenk H R 2006 *Science* **311** 644
[43] Wenk H R, Ischia G, Nishiyama N, Wang Y and Uchida T 2005 *Phys. Earth Planet. Inter.* **152** 191
[44] Loubeyre P, LeToullec R, Hausermann D, Hanfland M, Hemley R J, Mao H K and Finger L W 1996 *Nature* **383** 702
[45] Mao H K, Jephcoat A P, Hemley R J, Finger L W, Zha C S, Hazen R M and Cox D E 1988 *Science* **239** 1131
[46] Dera P, Zhuravlev K, Prakapenka V, Rivers M L, Finkelstein G J, Grubor-Urosevic O, Tschauner O, Clark S M and Downs R T 2013 *High Pressure Res.* **33** 466
[47] Li H, Li X D, He M, Li Y C, Liu J, Shen G and Zhang Z 2013 *J. Appl. Cryst.* **46** 387
[48] Ballaran T B, Kurnosov A and Trots D 2013 *High Pressure Res.* **33** 453
[49] Shen G, Ikuta D, Sinogeikin S, Li Q, Zhang Y and Chen C 2012 *Phys. Rev. Lett.* **109** 205503
[50] Li R, Liu J, Bai L G, Tse J S and Shen G 2015 *Appl. Phys. Lett.* **107** 072109
[51] Smith J S, Sinogeikin S V, Lin C L, Rod E, Bai L G and Shen G 2015 *Rev. Sci. Instrum.* **86** 072208
[52] Shen G, Duffy T S, Rivers M L, Eng P J, Sutton S R and Wang Y 1998 *Rev. High Pressure Sci. Technol.* **7** 1529
[53] Dhaussy A C, Mezouar M and Mentre O 2004 *AIP Conf. Proc.* **705** 1217

[54] Shen G, Prakapenka V B, Eng P J, Rivers M L and Sutton S R 2005 *J. Synchrotron. Rad.* **12** 642

[55] Mezouar M, Crichton W A, Bauchau S, Thurel F, Witsch H, Torrecillas F, Blattmann G, Marion P, Dabin Y, Chavanne J, Hignette O, Morawe C and Borel C 2005 *J. Sync. Rad.* **12** 659

[56] Shen G, Chow P, Yuming Xiao Y, Sinogeikin S, Meng Y, Yang W, Liermann H P, Shebanova O, Rod E, Bommannavar A and Mao H K 2008 *High Pressure Res.* **28** 145

[57] Lai B, Yun W, Xiao Y, Yang L, Legnini D, Cai Z, Krasnoperova A, Cerrina F, DiFabrizio E, Grella L and Gentili M 1995 *Rev. Sci. Instrum.* **66** 2287

[58] DiFabrizio E, Gentili M, Grella L, Baciocchi M, Krasnoperova A, Cerrina F, Yun W, Lai B and Gluskin E 1994 *J. Vac. Sci. Tec. B* **12** 3979

[59] Kirkpatrick P and Baez A V 1948 *J. Opt. Soc. Am.* **38** 766

[60] Underwood J H and Turner D 1977 *Proc. SPIE* **106** 125

[61] Thompson A C, Chapman K L, Ice G E, Sparks C J, Yun W, Lai B, Leginni D, Viccaro P J, Rivers M L, Bilderback D H and Thiel D J 1992 *Nucl. Instrum. Methods A* **319** 320

[62] Yang B X, Rivers M L, Schildkamp W and Eng P J 1995 *Rev. Sci. Instrum.* **66** 2278

[63] Eng P J, Newville M, Rivers M L and StSutton S R 1998 *SPIE Proc.* **3449** 145

[64] Yan H, Conley R, Bouet N and Chu Y S 2014 *J. Phys. D: Appl. Phys.* **47** 263001

[65] Snigirev A, Kohn V, Snigireva I and Lengeler B 1996 *Nature* **384** 7

[66] Che R Z, Zhou L, Zhao Y C, Gu H C, Wang Z J, Li F Y, Wang J F and Chen L C 1994 *Chin. Sci. Bull.* **39** 1877

[67] Liu J, Zhao J, Che R Z and Yang Y 2000 *Chin. Sci. Bull.* **45** 1659

[68] Tang L Y, Liu J, Xiao W S, Li Y C, Li X D and Bi Y 2010 *Chin. Phys. Lett.* **27** 016402

[69] Lin C L 2013 *Structural Phase Transitions in Rare ABO_3 Compounds and Gallium Garnet at High Pressure and High Temperature* (Ph. D. dissertation) (Beijing: Institute of High Energy Physics) (in Chinese)

[70] Bai L G 2010 *Phase Transitions and Equation of States of Rare Earth Sesquioxides* (Ph. D. dissertation) (Beijing: Institute of High Energy Physics) (in Chinese)

[71] Tsuji K, Yaoita K, Imai M, Shimomura O and Kikegawa T 1989 *Rev. Sci. Instrum.* **60** 2425

[72] Meade C, Hemley R J and Mao H K 1992 *Phys. Rev. Lett.* **69** 1387

[73] Kono Y, Park C, Kenney-Benson C, Shen G and Wang Y 2014 *Phys. Earth Planet. Inter.* **228** 269

[74] Lundegaard L F, Weck G, McMahon M I, Desgreniers S and Loubeyre P 2006 *Nature* **443** 201

[75] Mao H K, Hemley R J, Wu Y, Jephcoat A P, Finger L W, Zha C S and Bassett W A 1998 *Phys. Rev. Lett.* **60** 2649

[76] Zhang L, Meng Y, Dera P, Yang W, Mao W L and Mao H K 2013 *Proc. Natl. Acad. Sci.* **110** 6292

[77] McMahon M I, Loa I, Stinton G W and Lundegaard L F 2013 *High Pressure Res.* **33** 485

[78] Li R 2015 *Development and Application of High Pressure Single Crystal Diffraction and Multigrain Diffraction* (Ph.D. dissertation) (Beijing: Institute of High Energy Physics) (in Chinese)

[79] Singh A K and Kennedy G C 1974 *J. Appl. Phys.* **45** 4686

[80] Kinsland G L and Bassett W A 1977 *J. Appl. Phys.* **48** 978

[81] Duffy T S, Mao H K and Hemley R J 1995 *Phys. Rev. Lett.* **74** 1371

[82] Uchida T, Funamori N and Yagi T 1996 *J. Appl. Phys.* **80** 739

[83] Amulele G M, Manghnani M H and Somayazulu M 2006 *J. Appl. Phys.* **99** 023522

[84] Xiong L, Liu J, Bai L G, Li Y C, Lin C L, He D W, Peng F and Lin J F 2013 *J. Appl. Phys.* **113** 033507

[85] Mao H K, Shu J, Shen G, Hemley R J, Li B and Singh A K 1998 *Nature* **396** 741

[86] Duffy T S, Shen G, Jinfu Shu J, Mao H K, Hemley R J and Singh A K 1999 *J. Appl. Phys.* **86** 6729

[87] He D W and Duffy T S 2006 *Phys. Rev. B* **73** 134106

[88] Kiefer B, Shieh S R, Duffy T S and SekineT 2005 *Phys. Rev. B* **72** 014102

[89] Singh A K and Liermann H P 2011 *J. Appl. Phys.* **109** 113539

[90] Shieh S R, Duffy T S and Li B S 2002 *Phys. Rev. Lett.* **89** 255507

[91] Chen H, He D, Liu J, Li Y, Peng F, Li Z, Wang J and Bai L 2010 *Eur. Phys. J. B* **73** 321

[92] Xiong L 2014 *Investigations of Equation of State, Strength and Texture of Materials using Radial x-ray Diffraction Technique* (Ph. D. dissertation) (Beijing: Institute of High Energy Physics) (in Chinese)

[93] Xiong L, Liu J, Bai L G, Lin C L, He D W, Zhang X X and Lin J F 2015 *J. Alloys Compd.* **621** 116

[94] Xiong L, Liu J, Zhang X X, Tao Q and Zhu P W 2015 *J. Alloys Compd.* **623** 442

[95] Schultz E, Mezouar M, Crichton W. Bauchau S, Blattmann G, Andrault D, Fiquet G, Boehler R, Rambert N, Sitaud B and Loubeyre P 2005 *High Pressure Res.* **25** 71

[96] Prakapenka V B, Kubo A, Kuznetsov A, Laskin A, Shkurikhin O, Dera P, Rivers M L and Sutton S R 2008 *High Press. Res.* **28** 225

[97] Mao H K, Hemley R J, Gramsch S A, Shen G and Somayazulu M 2001 *Rev. Sci. Instrum.* **72** 1302

[98] Lin C L, Liu J, Lin J F, Li X D, Li Y C, Zhang Q L, Xiong L and Li R 2013 *Inorg. Chem.* **52** 431

[99] Mao H K, She G, Hemley R J and Duffy T S 1998 *Properties of Earht and Planetary materials at High Pressure and Temperature* (Washington, DC: AGU) p. 27

[100] Shen G and Heinz D L 1998 *Ultrahigh-Pressure Mineralogy: Physics and Chemistry of the Earth's Deep Interior* (Washington, DC: Mineralogical Society of America) p. 369

[101] Ma Y, Somayazulu M, Mao H K, Shu J, Shen G and Hemley R J 2004 *Phys. Earth Planet. Inter.* **143/144** 455

[102] Shen G, Prakapenka V B, Rivers M L and Sutton S R 2004 *Phys. Rev. Lett.* **92** 185701

[103] Cadien A, Hu Q Y, Meng Y, Cheng Y Q, Chen M W, Shu J F, Mao H K and Sheng H W 2013 *Phys. Rev. Lett.* **110** 125503

[104] Dera P, Finkelstein G J, Duffy T S, Downs R T, Meng Y, Prakapenka V B and Tkachev S 2013 *Phys. Earth Planet. Inter.* **221** 15

[105] Shen G, Mao H K, Hemley R J, Duffy T S and Rivers M L 1998 *Geophys. Res. Lett.* **25** 373

[106] Shen G, Sata N, Rivers M L and Sutton S R 2001 *Appl. Phys. Lett.* **78** 3208

[107] Dewaele A, Mezouar M, Guignot N and Loubeyre P 2010 *Phys. Rev. Lett.* **104** 255701

[108] Anzellini S, Dewaele A, Mezouar M, Loubeyre P and Morard G 2013 *Science* **340** 464

[109] Gregoryanz E, Sanloup C, Somayazulu M, Badro J, Fiquet G, Mao H K and Hemley R J 2004 *Nat. Mat.* **3** 294

[110] Crowhurst J C, Goncharov A F, Sadigh B, Evans C L, Morrall P G, Ferreira J L and Nelson A J 2006 *Science* **311** 1275

[111] Young A F, Sanloup C, Gregoryanz E, Scandolo S., Hemley R J and Mao H K 2006 *Phys. Rev. Lett.* **96** 155501

[112] Lavina B, Dera P, Kim E, Meng Y, Downs R T, Weck P F, Sutton S R and Zhao Y 2011 *Proc. Natl. Acad. Sci.* **108** 17281

[113] Fiquet G, Andrault D, Dewaele A, Charpin T, Kunz M and Hausermann D 1998 *Phys. Earth Planet. Inter.* **105** 21

[114] Shim S H, Duffy T S and Shen G 2000 *J. Geophys. Res.* **105** 25955

[115] Seagle C T, Campbell A J, Heinz D L, Shen G and Prakapenka V B 2006 *J. Geophys. Res.* **111** B06209

[116] Dorfman M, Meng Y, Prakapenka V B and Duffy T S 2013 *Earth Planet. Sci. Lett.* **361** 249

[117] Lin C L, Li Y C, Li X D, Li R, Lin J F and Liu J 2013 *J. Appl. Phys.* **114** 163521

[118] Lin C L, Zhang Y F, Liu J, Li X D, Li Y C, Tang L Y and Xiong L 2012 *J. Phys.: Condens. Matter* **24** 115402

[119] Lin C L, Liu J, Li X D, Li Y C, Chu S Q, Xiong L and Li R 2012 *J. Appl. Phys.* **112** 113512

[120] Sørensen H O, Schmidt S, Wright J P, Vaughan G BM, Techert S, Garman E F, Oddershede J, Davaasambu J, Paithankar K S, Gundlach C, Henning F and Poulsen H F 2012 *Z. Kristallogr.* **227** 63

[121] Zhang L, Meng Y, Yang W G, Wang L, Mao W L, Zeng Q S, Jeong J S, Wagner A J, Mkhoyan K A, Liu W J, Xu R Q and Mao H K 2014 *Science* **344** 877

[122] Evans W J, Yoo C S, Lee G W, Cynn H, Lipp M J and Visbeck K 2007 *Rev. Sci. Instrum.* **78** 073904

[123] Goncharov A F, Prakapenka V B, Struzhkin V V, Kantor I, Rivers M L and Dalton D A 2010 *Rev. Sci. Instrum.* **81** 113902

[124] Meng Y, Hrubiak R, Rod E, Boehler R and Shen G 2015 *Rev. Sci. Instrum.* **86** 072201